Sensors & Actuators: B. Chemical 344 (2021) 130194

Contents lists available at ScienceDirect

Sensors and Actuators: B. Chemical

journal homepage: www.elsevier.com/locate/snb

Eu-Coordinated semiconducting polymer nanoparticles as a novel nanoprobe with two detection method signals for determination of copper (II) ions

Xiao Liu [1], Juan Han [1], Xu Wu *, David Pierce *, Julia Xiaojun Zhao *

Department of Chemistry, University of North Dakota, Grand Forks, ND 58202, USA

ARTICLE INFO

Keywords:
Two-readout
Single particle ICP-MS
Fluorescence
Semiconducting polymer nanoparticles
Copper ion

ABSTRACT

Eu-coordinated semiconducting polymer nanoparticles (SPNs-Eu) were developed for bimodal analysis of copper (II) ions (Cu^{2+}) over a wide dynamic range (μM to pM). In this sensing system, the first readout mode is based on the fluorescence signal of SPNs-Eu. A significant quenching of the fluorophore is selective for the presence of Cu^{2+} due to the aggregation of SPNs-Eu. The aggregations are caused by chelation of Cu^{2+} with carboxylate groups on SPNs-Eu and the amount of aggregation can be quantified by the ^{153}Eu signal of SPNs-Eu using single-particle inductively coupled plasma mass spectrometry (sp-ICPMS). This signal is the second readout mode of these nanoparticles, which can be calibrated for sub-pM determination of Cu^{2+}. Compared with the monodisperse SPNs-Eu reagent, aggregation in the presence of Cu^{2+} significantly decreases the number of detected particles or particle clusters within a sampling period of the sp-ICPMS measurement. The fluorescence readout yields a facile and rapid detection method with a rather limited linear range from 2 μM to 50 μM and a limit of detection (LOD) of 0.29 μM. In contrast, the sp-ICPMS readout provides a far more sensitive analysis method with a linear range from 1 pM to 10 μM and a LOD of 0.42 pM.

1. Introduction

A series of spectroscopic methods, including atomic absorption/emission spectrometry (AAS/AES), inductively coupled plasma mass spectrometry (ICPMS), fluorescence spectrometry etc., have been developed to satisfy different requirements or scenarios of analysis [1–6]. Basically, most of the approaches choose a specific signal to quantify the amount of analyte. For example, the mass spectrometry focused on the masses of analytes to obtain the concentration information [7]. The colorimetry collects the absorption of light to evaluate the content of analyte [8]. However, given the instinct disadvantages in each method, all the information obtained from one signal is insufficient to meet the requirement of accuracy, repeatability, and limit of detection in a complicated condition with high background noise or low analyte concentration. To overcome the proposed problems, researchers have introduced more signals in one method of the corresponding sensing system. For example, a group of ratiometric optical oxygen sensing probes were designed to contain two signals, which could be achieved by a dual emission signal involved system with two different luminophores, one emits oxygen-insensitive fluorescence as reference peak and the other emits oxygen-quenchable phosphorescence [9]. The extra signal of reference peak generates superiorities including high sensitivity as well as inherent reliability [9]. Furthermore, dual signal sensors have also been applied in electrochemical analysis and bioimaging. Combining ferrocene and thionine current readout together, Hou's group designed a dual-signal aptamer sensor which exhibited high sensitivity to malathion [10]. Up to now, most of the improvements were chosen to bring in more signals to create more information for data analysis within one settled detection method. However, if the method itself has instinctive limitations, this idea might have little break through on the limit of detection and dynamic range. Therefore, scientists tended to merge signals from various methods together. For example, combining magnetic resonance imaging (MRI) with fluorescent molecular tomographic (FMT), Chen's group could obtain both three-dimensional multimodal images of living mouse brains and monitor the tumor morphology as well as protease activity [11]. Xu et al. designed a dual-readout biosensor that combined the colorimetric signal and photothermal signal together to quantify a tumor biomarker. The

* Corresponding authors.
E-mail addresses: Xu.wu@und.edu (X. Wu), Pierce.David@und.edu (D. Pierce), Julia.zhao@und.edu (J.X. Zhao).
[1] The first two authors contribute equally to this work.

https://doi.org/10.1016/j.snb.2021.130194
Received 8 February 2021; Received in revised form 24 May 2021; Accepted 26 May 2021
Available online 27 May 2021

Table 1
Operation parameters used for sp-ICPMS measurements.

Parameters	Value
Radio frequency power (W)	1550.00
Cooling gas flow rate (L min^{-1})	14.00
Nebulizer gas flow rate (L min^{-1})	1.09
Spray chamber temperature (°C)	2.70
Sampling depth	5.00
Peristaltic pump speed (rpm)	20.00

two signals from this biosensor not only validated each other to improve the accuracy and reliability of the test, but also provide the two approaches for determination under different conditions. Colorimetric analysis could be performed by eye with low sensitivity but the photothermal signal provided significantly enhance sensitivity for trace analysis [12]. Recently, Chiu's group developed a lanthanide-coordinated semiconducting polymer dots for single cell analysis using flow cytometry and mass cytometry with both fluorescence and mass readouts, respectively. The advantages of these dual-readout probes included the capability of rapid and sensitive cell analysis by flow cytometry and multiplex analysis by mass cytometry [13]. Moreover, integration of the fluorescence and ICP-MS signals of these bimodal probes allowed a more thorough and precise discrimination of the target analytes in a complex sample matrix.

Fluorometric analysis has been regarded as a rapid and simple method for metal-ion determination. A wide range of fluorescent probes have been used in this field, such as organic dye molecules, quantum dots, nanoclusters and semiconducting polymer dots [14,15]. The procedure of fluorometric analysis is flexible and can be performed with low-cost instruments. Therefore, it is suitable for quick quantification and field-screening applications, such as monitoring the toxic metals in environmental samples [16]. However, it is a noticeable disadvantage that fluorometric analysis of metal ions is relatively low sensitivity, narrow detection range, and background interference from the sample matrix. In contrast, single particle inductively coupled plasma-mass spectrometry (sp-ICPMS) has been reported as a promising analytical approach for the analysis of metal-containing nanoparticles albeit coupled with more complex sample preparation and relatively high cost. The technology of sp-ICPMS is originally from the regular ICPMS, which shows excellent features of the regular ICPMS including ultra-high sensitivity, broad dynamic range, and low limit of detection for the analysis. More importantly, it could also provide comprehensive information on the physical properties of nanoparticles such as size, size distribution, particle density, particle number concentration, and aggregate status in solution [17]. In the profile of the sp-ICPMS measurement for this work, the signal for a single particle (SPN-Eu) is measured as a single pulse within the time-based data set. Consequently, the number of pulses detected within the set is dependent on the concentration of the nanoparticles or nanoparticle clusters in the sample. Moreover, the count intensity of the pulse is directly proportional to the amount of metal element doped in a single nanoparticle or present in the nanoparticle cluster. Because sp-ICPMS is a "particle by particle" detection process, the particle solutions are analyzed at an extremely low concentration, which provides high sensitivity for any target-specific aggregation of the nanoparticle probes. Typically, the number of detected pulses decreases while pulse intensity concomitantly increases compared to the original probe solution. However, if the probe agglomeration is severe and clusters precipitate from the solution, only a decreased pulse number will be observed because the precipitated clusters will not be introduced into the sp-ICPMS.

Inspired by the previous work of the trace analysis and the above-mentioned technology, the signal of fluorometric methods and the signal sp-ICPMS could be merge together as a two readout nanoprobe. To the best of our knowledge, this two-readout metal-containing polymer nanoparticles based on the technology of fluorometry and sp-ICPMS for metal ion analysis has not been reported. In this system, Eu-coordinated fluorescent semiconducting polymer nanoparticles not only provide a fluorescence quenching signal due to aggregation induced by the target ion, but also offer an ^{153}Eu signal by the sp-ICPMS. Compared to other types of metal elements, such as alkali metals and transition metals, investigated by sp-ICPMS, the instrument is more sensitive to rare lanthanide elements due to their seldom found in the earth. To test the applicability of this two-readout nanoprobe, the copper(II) ion (Cu^{2+}) was chosen as a target analyte. Copper, as an essential human nutrient, is involved in various physiological functions in biological activities, especially in cell generation and enzymatic processes [18,19]. However, copper at high levels caused deleterious physiological effects [20–22] and its environmental contamination has been considered as a serious safety issue due to its wide and long-term effect [23,24].

For copper detection, there are already plenty of well-known methods, such as, atomic absorption spectra, surface plasma resonance, colorimetric assay, electrochemistry methods, DNA enzyme methods, and fluorometric detection [25–30]. Among all these single signal methods, this two-readout SPN-Eu sensing probe combined two method signals into one system, merging both fast and simple advantages from fluorometric methods, also uniting the accuracy and low LOD advantages from sp-ICPMS. In this way, the SPN-Eu has broken through the limitations of mono modal signal sensor in some perspectives of sensitivity, dynamic range and limit of detection.

In this article, Eu^{3+}-coordinated MEH-PPV semiconducting polymer nanoparticles (SPNs-Eu) were designed for the detection of Cu^{2+}. This nanoprobe SPN-Eu could be investigated under two different methods. One readout is the fluorescence signal emitted by SPNs composed of red fluorescent semiconducting polymer, MEH-PPV. The other readout is based on the Eu mass signal from the Eu^{3+} coordinated on the PSMA polymer. In the presence of Cu^{2+}, efficient chelating between the carboxylate groups on SPNs-Eu and Cu^{2+} results in the aggregation of SPNs-Eu, which induces a significant fluorescence quenching as well as a decreased in nanoparticle pulses detected in the sp-ICPMS profile. Therefore, both the fluorescence and sp-ICPMS signals are responsive to the concentration of Cu^{2+}.

2. Experimental sections

2.1. Materials and instruments

Poly[2-methoxy-5-(2-ethylhexyloxy)-1,4-phenylenevinylene] (MEH-PPV, average molecular weight is 40,000–70,000 Da), poly (styrene-co-maleic anhydride) (PSMA), europium(III) chloride, 4-(2-hydroxyethyl)piperazine-1-ethanesulfonicacid (HEPES, 99.5 %, ACS grade), copper(II) sulfate, potassium chloride, sodium chloride, magnesium(II) sulfate, zinc(II) sulfate, manganese(II) dichloride, lead(II) sulfate and tetrahydrofuran (THF, 99.9 %, inhibitor-free, ACS grade) were purchased from Sigma Aldrich Inc. Deionized (DI) water (18.2 MΩ·cm) used in all experiments was obtained using a Milli-Q Millipore water purification system.

A UV/VIS/NIR spectrometer (Lambda 1050, PerkinElmer) was used to measure the absorption spectra of samples. Fluorescence measurements were performed on a RF-6000 fluorophotometer (Shimadzu, Japan). The excitation wavelength was set to be 480 nm and the emission was recorded from 500 nm to 700 nm. The fluorescence intensity at 560 nm was selected to evaluate the performance of SPNs-Eu probe for copper ion detection. The widths of excitation and emission slits were set as 10.0 nm. All the experiments were carried out at room temperature. A Zetasizer particle analyzer (Nano-ZS, Malvern) was used to measure hydrodynamic diameters and surface charges of nanoparticles. A Hitachi 7500 transmission electron microscope (Hitachi, Tokyo, Japan) was used to obtain the morphology of the synthesized nanoparticles. A FTIR Spectrum ATR iD5 spectrometer (ThermoFisher Scientific, Waltham, UK) was used to collect the Fourier transform infrared (FTIR) spectra of

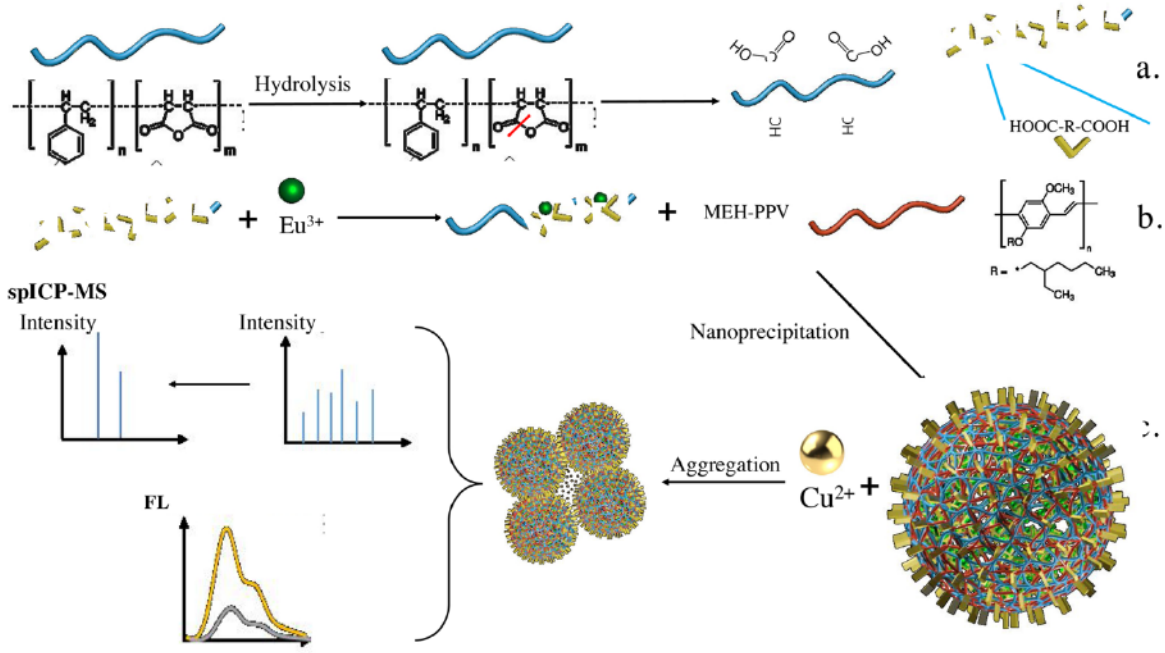

Scheme 1. Schematic illustration of the preparation of SPNs-Eu for the detection of Cu^{2+}.

SPN-Eu.

An iCAP Qc ICPMS (Thermo Scientific, Bremen, Germany) was used for all sp-ICPMS measurements. Samples were introduced using a Teledyne CETAC ASX560 autosampler (Omaha, NE), a 4-channel 12-roller peristaltic pump, a microflow perfluoroalkoxy nebulizer and a Peltier-cooled quartz cyclonic spray chamber. The sample flow rate was set to be ~ 0.20 mL/min. The ICPMS was tuned daily for maximum ^{238}U and minimum $^{140}Ce^{16}O/^{140}Ce$ oxide level (< 0.03) with THERMO-4AREV (Thermo Scientific) standard solution in STDs mode. Detailed information about the sp-ICPMS operation parameters were provided in Table 1. The dwell time and data collection time for all the sp-ICPMS measurements were 10 ms and 180 s. Isotope ^{153}Eu intensity was recorded using Qtegra™ software (version 2.8.2944.202).

2.2. Synthesis of the SPNs-Eu

To prepare the SPNs-Eu, PSMA requires a pre-treatment to form the carboxyl groups. Briefly, 0.05 g PSMA was dissolved into 1.0 mL THF followed by injecting into an aliquot of 10 mL water. With mild stirring, the above solution was dried to collect white powder, which was designated as PSMA-COOH. After that, the powder was re-dissolved into THF to produce a final solution of 1.0 mg/mL PSMA-COOH. For SPNs-Eu synthesis, an aliquot of 15 μL of $EuCl_3$ solution (10.0 mg/mL in THF/EtOH) was first mixed with 4.4 mL of THF, followed by adding 500.0 μL of 1.0 mg/mL PSMA-COOH solution and stirred for 2 h. Then, an aliquot of 50.0 μL of 0.5 mg/mL MEH-PPV polymer was added into the previous solution to reach the final volume of 5.0 mL. Finally, the mixed THF solution was quickly injected into 10.0 mL of DI water under ultrasonication in the ice bath for about 1.0 min. THF was evaporated through heating on a hot plate. The solution was filtered with a 0.45-μm cellulose membrane filter to remove the large aggregations. Lastly, the ultracentrifugation with 100 KDa cut-off was used to remove free metal ions from the SPNs-Eu and concentrate the solution.

2.3. Copper detection using the fluorometric method and sp-ICPMS

For Cu(II) detection using fluorometric method, an aliquot of final concentration of 1.0 mg/L of SPNs-Eu solution was incubated with different concentrations (0 μM, 2 μM, 5 μM, 10 μM, 20 μM, 40 μM, 50 μM, 60 μM and 80 μM) of copper ions for 1.0 h in a HEPES buffer solution (20 mM, pH 7.0) to reach a total volume of 1.0 mL at room temperature with regular shaking. Then, the fluorescence spectra of above solution were recorded at the excitation wavelength of 480 nm. The fluorescence intensity at 560 nm was plotted with the concentrations of copper ions. As for detecting Cu(II) using sp-ICPMS, the same aliquot of final concentration of 1.0 mg/L of SPNs-Eu solution was incubated with a series of extremely low concentrations (0, 1.0 pM, 10.0 pM, 100.0 pM, 1.0 nM, 10.0 nM, 100.0 nM, 1.0 μM, 10.0 μM, 100.0 μM, and 1.0 mM) for the same reaction time. Before injecting into the sp-ICPMS, the above prepared SPNs-Eu were addressed with a series of dilution. The mass concentration could be transferred into particle number concentration. The diameter of the SPN-Eu was determined by Zetasizer particle analyzer. Assuming the state of polymer nanoparticles are suspended in the solution (the density of SPN-Eu to be 1 mg/mL) and SPN-Eu is spheric, the volume of SPN-Eu could be calculated, thus the average molar mass (M) of SPN-Eu could be calculated ($M = N_A V\rho$). The mass concentration could be transferred into molarity and corresponding particle number concentration. After optimizing the particle number concentration, the known concentration should be diluted to 10^4 particles/mL with DI water.

2.4. Selectivity investigation for Cu^{2+} detection

With the fluorometric method, the selectivity of the SPNs-Eu on different metal ions was investigated by incubating a final concentration of 1.0 mg/L of SPNs-Eu solution (20 mM HEPES buffer, pH 7.0) with different metal ions (Co^{2+}, Fe^{3+}, Fe^{2+}, Pb^{2+}, Mg^{2+}, Cd^{2+}, Ag^{+}, Zn^{2+}, Al^{3+}, Mn^{2+}, and Cu^{2+}). The concentrations of the metal ions were fixed at 50 μM. After 1 h incubation at room temperature, the fluorescence spectra of the solutions were recorded. For the selectivity investigation with sp-ICPMS method, the samples were performed at the sample reaction condition but with a series of metal ions at the concentration of 1.0 μM. Before injecting into the sp-ICPMS, the concentration of SPNs-Eu was diluted down to 10^4 particles/mL with DI water.

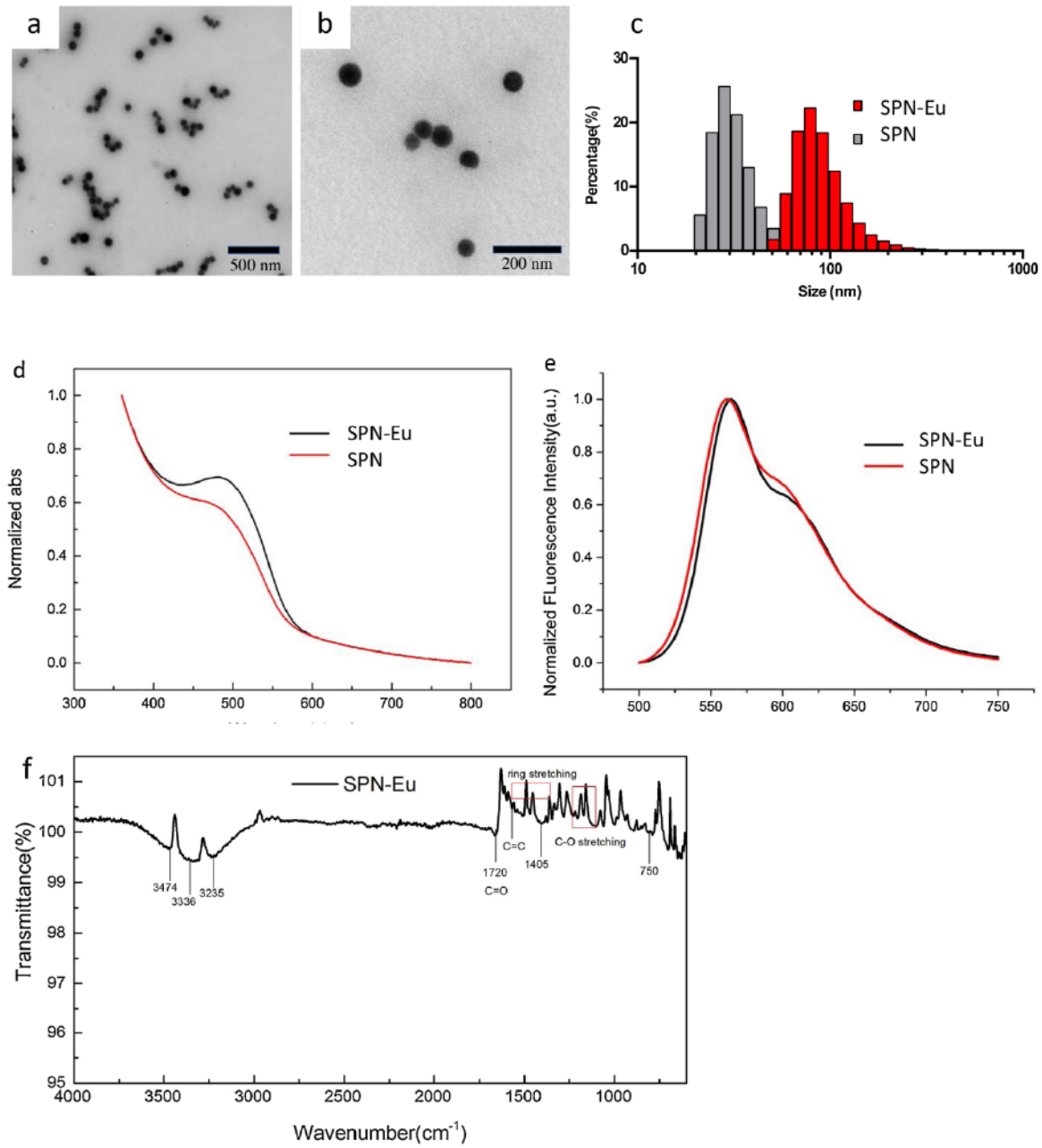

Fig. 1. (a) TEM image of SPNs-Eu (scale bar is 500 nm). (b) The enlarged TEM image of SPNs-Eu (scale bar is 200 nm). (c) Size distribution (pH 7.0, 20 mM HEPES) of SPNs and SPNs-Eu measured by DLS.(d) (A) Normalized Absorption of SPN and SPN-Eu. (e) Normalized emission spectra of SPN and SPN-Eu. (f) The FT-IR spectra of SPN-Eu.

3. Results and discussion

3.1. Design of the SPNs-Eu for Cu^{2+} detection

In this work, we designed an SPNs-Eu for Cu^{2+} detection with two readouts modes, including signals in fluorometric spectrometry and pulse signals in sp-ICPMS. To construct the SPNs-Eu nanoprobe, poly (styrene-co-maleic anhydride) (PSMA) was first hydrolyzed to form the carboxyl-functionalized polymer (PSMA-COOH), then followed by adding $EuCl_3$ THF/ethanol solution with vigorous stirring for 2 h (Scheme 1a). During this period, PSMA served as a highly efficient absorbent, Europium ions could be chelated with PSMA-COOH through the abundant carboxyl groups [13]. After the immobilization, MEH-PPV polymer was blended into the above solution. After mixing with fluorescent MEH-PPV polymer in THF, the mixture was immediately injected into water to form SPNs-Eu (Scheme 1b). During the water injection process, the polymer chains of MEH-PPV and PSMA would shrink into ball-shaped nanoparticles due to the hydrophobic interaction, however, carboxylic groups would stay in the surface for their high hydrophilic properties.

As one of the rare metal elements, Eu^{3+} is suitable to be applied in sp-ICPMS analysis because of its low background signal. Compared with LOD of another transition metal element such as Ru (LOD: 3.00×10^{-3} μg/L), the LOD of sp-ICPMS instrument of rare earth element Eu is lower with 0.17×10^{-3} μg/L. Considering a suitable matrix to combine both sp-ICPMS signal and fluorescence signal, semiconducting polymer nanoparticles (SPNs) would be a great choice to fulfill the purpose. There are three main advantages for using SPNs. First, SPNs could be designed to contain a large amount of metal ions that would enhance the sp-ICPMS signal. Second, SPNs exhibit superior fluorescence properties,

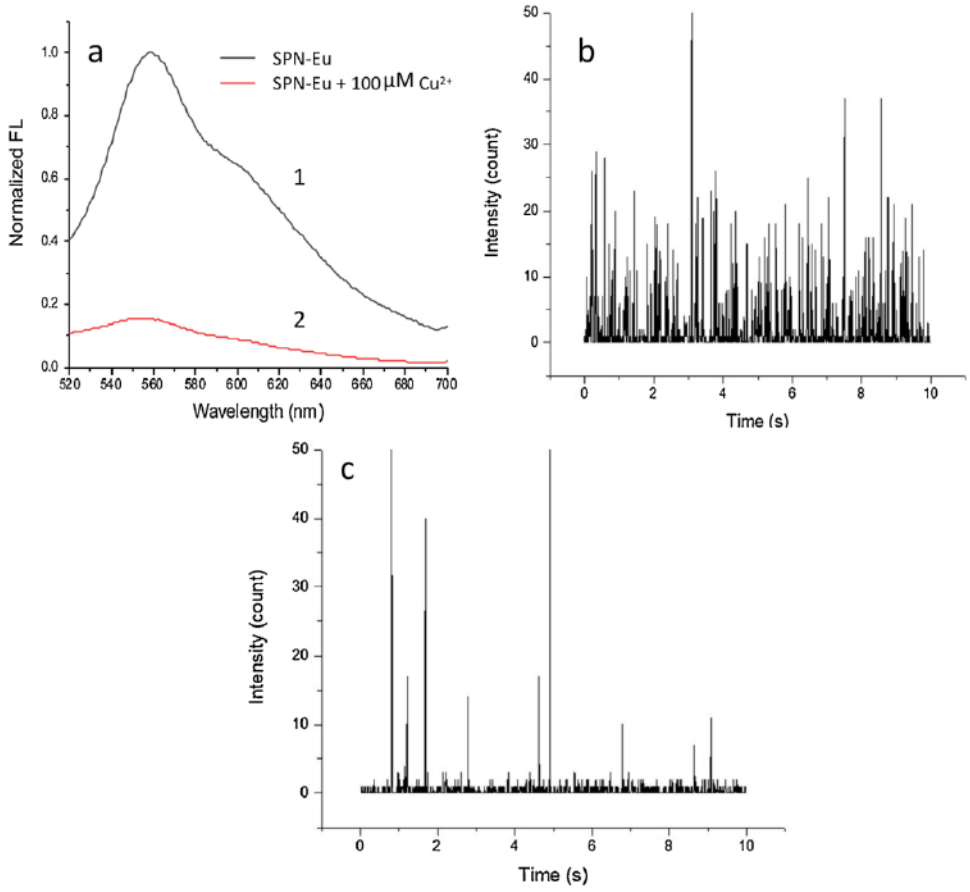

Fig. 2. (a) Fluorescence emission spectra of 1.0 mg/L SPNs-Eu without (curve 1) and with (curve 2) 100 μM Cu^{2+}. (λ_{ex} = 480 nm). sp-ICPMS profile of 1.0×10^4 P/mL SPNs-Eu without (b) and with (c) 100 μM Cu^{2+}. The signal of ^{153}Eu isotope was recorded in 180 s with a dwell time of 10 ms. The figures showed a period of 10s' spectra.

such as high quantum yield, large Stokes shift, and high photostability. Third, the synthetic process of lanthanide doped SPNs is simple, without a tedious synthesis protocol compared to other lanthanide-containing nanoparticles, such as upconversion nanoparticles [31]. Considering these features, a novel two-readout nanoprobe based on SPNs-Eu for Cu^{2+} detection was constructed.

Copper, as a pivotal metal in human life, is involved in various physiological functions in biological activities, especially in cell generation and enzymatic processes. However, copper exhibits high toxicity if over-ingested. For example, through the food chain, it will be a direct reason to cause multiple serious neurodegenerative diseases, such as Wilson and Parkinson's. Copper pollution has been considered as a serious safety issue due to its wide and long-term effect. Therefore, fast and sensitive detection of copper ions is highly significant. The mechanism of this novel nanoprobe is based on efficient chelating interactions between Cu(II) and carboxylic groups on the nanoparticles, which causes a significant fluorescence quenching. This could be explained by Irving-Williams series. Comparing with other transition metals, Cu^{2+} tends to form more stable bonding interactions the abundant carboxylic groups electron donors on the GQDs, which would cause aggregation accompanied with self-fluorescence quenching. It has been reported that carboxylic functional groups modified semiconducting polymer nanoparticles could also be quenched by Cu^{2+} through the same mechanism of strong interaction induced self-quenching [32,33]. As shown in Scheme 1c, in the presence of Cu^{2+}, SPNs-Eu started to aggregate together due the coordination interactions between the carboxyl groups on the surface of SPNs-Eu and Cu^{2+}. The aggregation process not only resulted in the fluorescence quenching of SPNs-Eu, but also decreased the spike numbers recorded in sp-ICPMS measurement, in which one spike stood for single nanoparticle or single aggregate unit. Using the variations of these two signals before and after the addition of Cu^{2+}, a two-readout sensing nanoprobe was fabricated for the detection of Cu^{2+}. We anticipated that these two readouts would be used in different scenarios due to their different detection sensitivities and costs. For the applications that require quick measurement and low-cost and compatible with low sensitivity, the fluorescence readout might be the best option. However, for the accurate measurement of trace amount of Cu^{2+}, the sp-ICPMS method might be the one to use, which would ensure a lower detection limit and broad dynamic range. Therefore, we believe that this two-readout SPNs-Eu will provide comprehensive detection method for Cu^{2+} with different requirements.

3.2. Synthesis and characterization of SPNs-Eu

In our previous work, different lanthanide ions have been doped into SPNs composed of carboxyl-functionalized poly[(9,9-dioctylfluorenyl-2,7-diyl)-co-(1,4-benzo-{2,10,3}-thiadazole)] polymer to form the lanthanide-doped SPNs with the signals fluorescence and rare-earth isotopes [13]. However, the synthesis of carboxyl-modified semiconducting polymers were complicated and the fluorescence quantum yield of SPNs was sacrificed through the carboxyl modification. In order to solve the limitations of laborious synthesis and expand the fluorescent emission of the lanthanide-doped SPNs, a similar carboxyl-modified polymer structure was fabricated from the hydrolysis of PSMA, which could be obtained commercially at low-cost and be used to chelate with metal ions. This carboxyl-modified PSMA (PSMA-COOH) simplified the synthesis of SPNs-Eu through nanoprecipitation method. With this method, different fluorescent semiconducting polymer could be blended

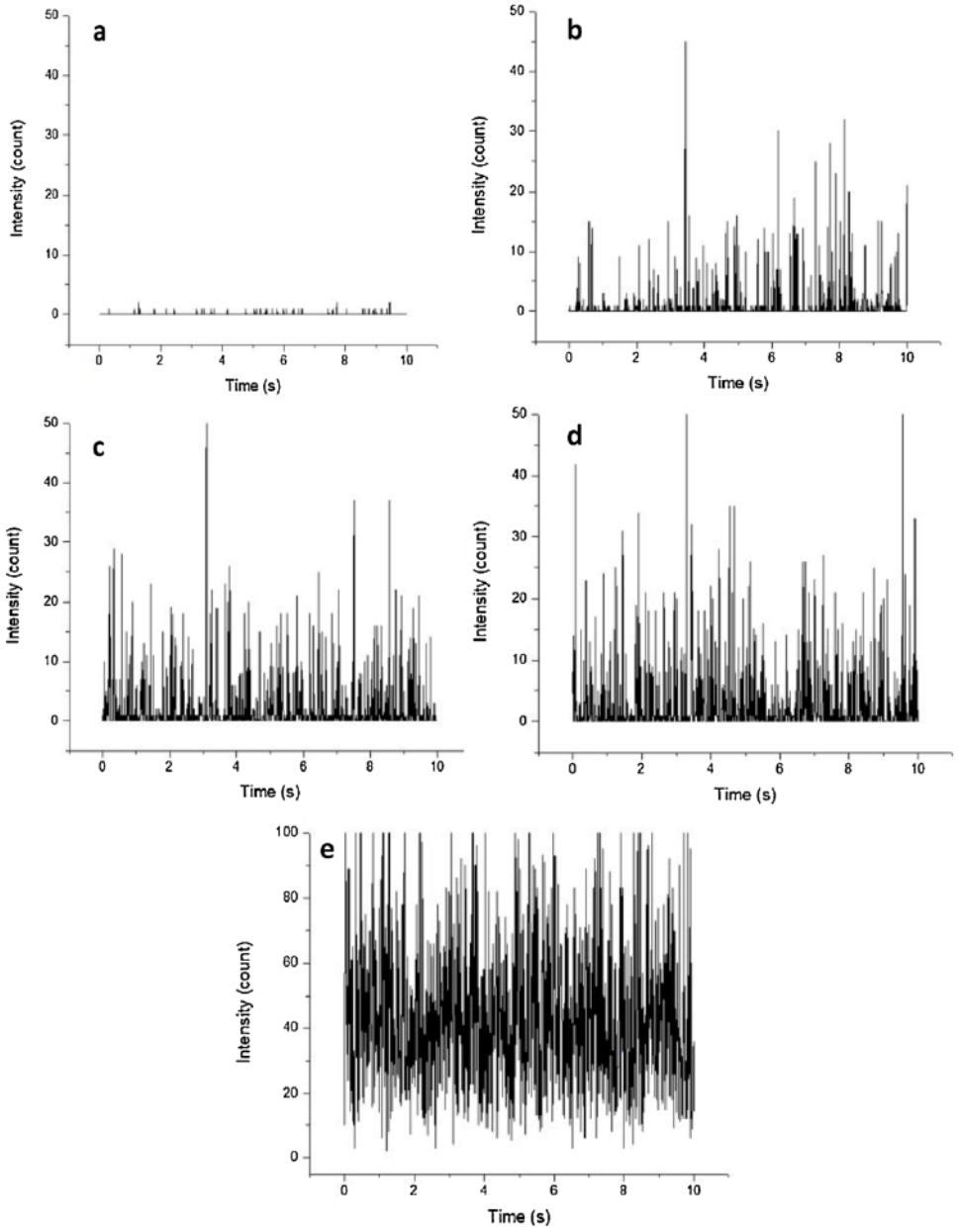

Fig. 3. sp-ICPMS profile of SPNs-Eu with different concentrations. (a: 0 P/mL, b: 5.0×10^3 P/mL, c: 1.0×10^4 P/mL, d: 2.0×10^4 P/mL, e: 5.0×10^4 P/mL). The signal of ^{153}Eu was recorded in 180 s with dwell time of 10 ms. The figures showed a period of 10s' spectra.

with PSMA-COO-Eu to form SPNs. In this work, we chose Poly [2-methoxy-5-(2-ethylhexyloxy)-1,4-phenylenevinylene] (MEH-PPV), a red color fluorescent polymer, as an example to prepare the SPNs-Eu. The morphology and size of SPNs-Eu was characterized with a regular transmission electron microscope (TEM) and dynamic light scattering (DLS). As shown in Fig. 1a and b, TEM images showed round-shaped, well-dispersed SPNs-Eu. The diameter of SPNs-Eu was measured to be 76.3 ± 11.1 nm from the TEM images. We found that the hydrodynamic diameter of SPNs-Eu was much larger that the pure SPNs without doping of Eu^{3+}. The SPNs-Eu showed a hydrodynamic diameter of 80.0 ± 2.7 nm, which is slightly larger than the diameter measured by TEM. The pure SPNs possessed a hydrodynamic diameter of 20.2 ± 0.2 nm, which is consistent with previous report. After optimizing the ratio between the Eu^{3+} and PSMA-COOH, we prepared the largest SPNs-Eu with the best stability, which provided the highest Eu^{3+} isotope signal from a single SPNs-Eu. Moreover, the zeta potential of SPNs-Eu and SPNs were measured to be both lower than −20 mV, we did the calculation of the carboxylic groups and Eu^{3+} in the PSMA-COOH used for the synthesis SPN-Eu. Under the optimized condition, the ratio between the COOH groups in the used PSMA-COOH and Eu^{3+} was calculated to be around 75:1, which means there would be a lot of free COOH groups in the synthesized SPN-Eu even all the Eu^{3+} had been coordinated into the SPN-Eu. Therefore, we believe the negative surface zeta potential not only come from the COOH groups, but also due to the oxygen related defects formed on the polymer chains during the process of forming nanoparticles, which assured the stability of the SPNs-Eu through the electrostatic repulsion. In Fig. 1(d), the absorption peak of SPN is overlapped by that of SPN-Eu, which implies the existence of the MEH-PPV polymer chain in SPN-Eu after nanoprecipitation, the feature peak is at 480 nm, which has been reported in other relative SPN research. In Fig. 1(e), the emission wavelength of both SPN and SPN-Eu was at 560 nm, which demonstrated that the source of the fluorescence signal is from MEH-PPV fluorescence polymer. FTIR of SPN-Eu was used to demonstrate the existence of various functional groups. As shown in

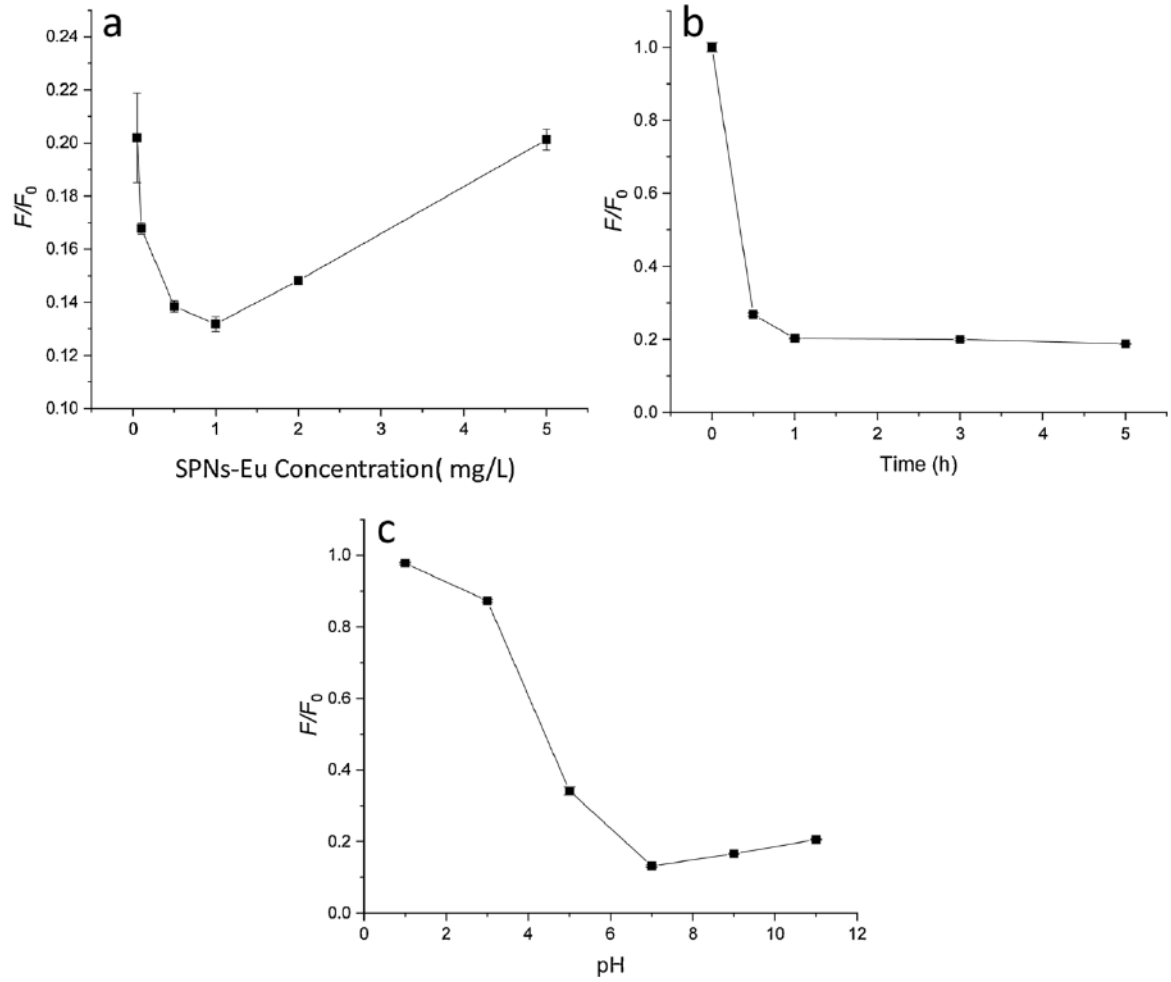

Fig. 4. Optimization of the reaction conditions. (a) The effect of concentration of SPNs-Eu on the sensitivity of the sensing nanoprobe. (b) The optimization of the reaction time for Cu^{2+} detection with 1.0 mg/L SPNs-Eu. (c) The effect of pH on the sensitivity of SPNs-Eu for Cu^{2+} detection. The concentration of SPNs-Eu was 1.0 mg/L and reaction time was 1 h. In all the figures, F_0 referred to the fluorescence intensity SPNs-Eu in 20 mM HEPES buffer. F referred to the fluorescence intensity of SPNs-Eu treated with 100 μM Cu^{2+} in 20 mM HEPES buffer. λ_{ex} = 480 nm, λ_{em} = 560 nm.

Fig. 1f, the peaks at 750 cm^{-1}, 1250 cm^{-1}, 1500 cm^{-1} suggested the presence of the C—H bending, CO— stretching and ring stretching in SPN-Eu. The presence of C═C non-aromatic bonds was proved by the broad peak area at 1600 cm^{-1} and the presence of C═O bonds was showed in the sharp peak at 1720 cm^{-1}. The CO═ bonds on the anhydride rings is flat, which demonstrate most of the anhydride rings have hydrolyzed and chelated with Eu^{3+}; These stretching vibration peaks at 3200 – 3500 cm^{-1} has been reported, which demonstrate the existence of MEH-PPV polymer.

3.3. Feasibility investigation of Cu^{2+} detection

After we prepared and characterized the SPNs-Eu, we investigated the fluorescence intensity response and variation of spike numbers in sp-ICPMS of SPNs-Eu before and after the addition of Cu^{2+}. As shown in Fig. 2a, the fluorescence intensity of SPNs-Eu decreased by about 82 % in the presence of 100 μM Cu^{2+}. Also, the response of SPNs-Eu to Cu^{2+} was also investigated by the sp-ICPMS method (Fig. 2b & c). The results showed that the spike numbers in the 180 s collection time decreased from 3590 to 864 in the presence of 100 μM Cu^{2+}. Obviously, there was about 76 % decrease of the spike numbers detected in the sp-ICPMS method. The results demonstrated the feasibility of SPNs-Eu nanoprobe for Cu^{2+} detection in these two detection modes.

3.4. Optimization of the concentration of SPNs-Eu for sp-ICPMS measurement

The concentration of nanoparticles injected into the sp-ICPMS is extremely important to obtain the best sensitivity and accuracy. If the concentration is too low, not enough single particle events will be collected in a certain period of collection time. However, if the concentration is too high, continuous signals were collected, of which a single spike in each dwell time might stand for multiple events rather than one individual event. Also, the background noise might be increased, which decreased the sensitivity of the method. Therefore, we optimized the injecting concentration of SPNs-Eu for sp-ICPMS measurement. As shown in Fig. 3, a series of concentration of SPNs-Eu including 0, 5.0 × 10^3, 1.0 × 10^4, 2.0 × 10^4 to 5.0 × 10^4 P/mL was introduced into the sp-ICPMS, and each sample was collected for 180 s with a dwell time of 10 ms. With the increasing of particle number concentration of SPNs-Eu, the number of spike peaks increased as well. However, when the concentration of SPNs-Eu was equal or higher than 2.0 × 10^4 P/mL, multiple nanoparticles were observed in each dwell time, indicated by the continuous spikes instead of individual spikes. Furthermore, when the concentration reached 5.0 × 10^4 P/mL, the baseline from isotope Eu dramatically increased as well, showing the enhanced background noise in the measurement. From this tendency, we found out that increasing the particle number concentration introduced in the plasma would increase the signals from dissolved Eu ions.

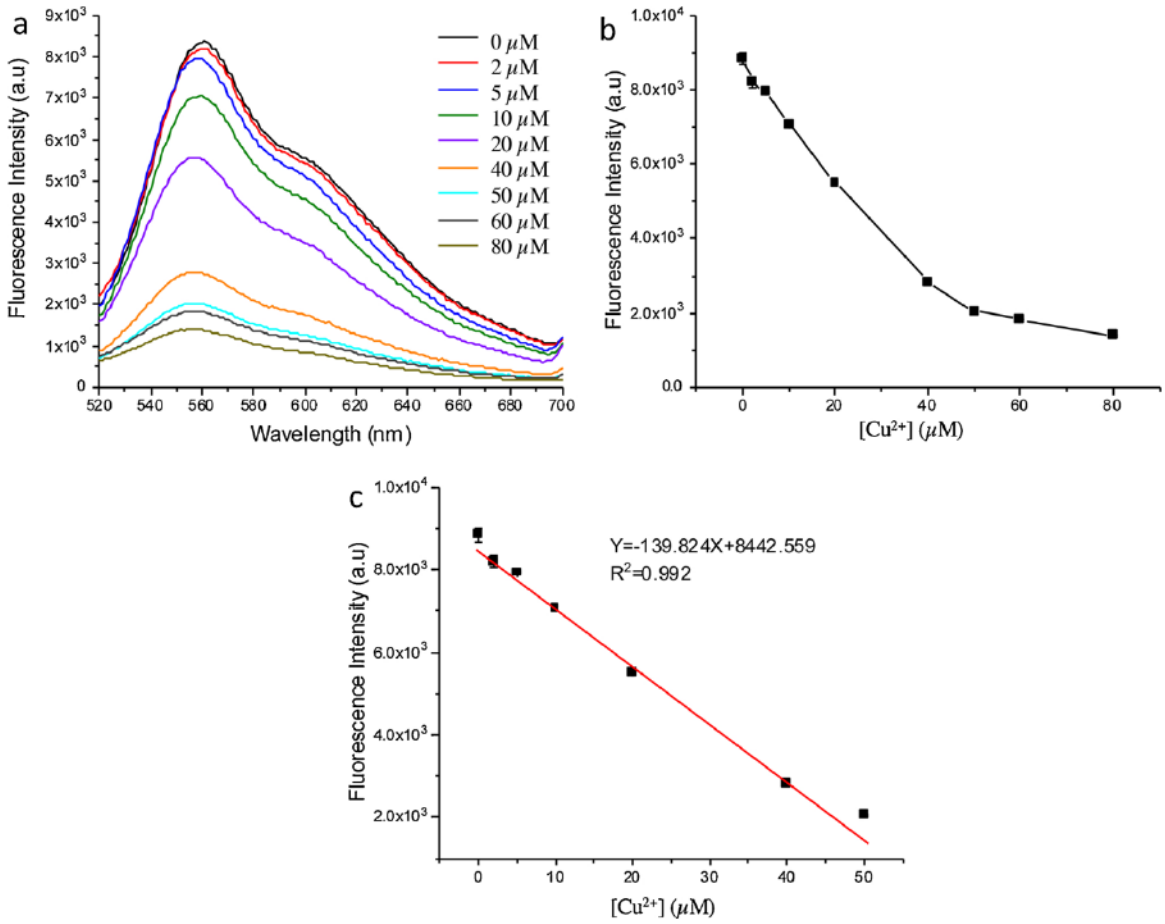

Fig. 5. (a) Fluorescence spectra of SPNs-Eu (1.0 mg/L) in the presence of various concentrations of Cu^{2+} (0, 2, 5, 10, 20, 40, 50, 60 and 80 μM). λ_{ex} = 480 nm, λ_{em} = 520 nm – 700 nm. (b) Relationship between the relative fluorescence intensity at 560 nm and concentrations of Cu^{2+}. (c) Calibration curve of the fluorescence intensity of SPNs-Eu Cu^{2+} detection in the range of 1 – 50 μM.

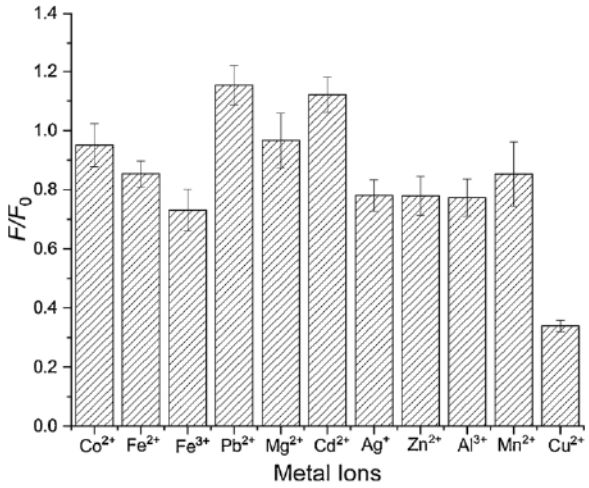

Fig. 6. The fluorescence responses of the SPNs-Eu (1.0 mg/L) to various metal ions (50 μM) and Cu^{2+} (50 μM) in 20 mM HEPES solution (pH 7.0).

Considering the interference from dissolved Eu ions and the identification of particle events in signals, the sp-ICPMS profile of SPNs-Eu with the concentration of 1.0×10^4 P/mL obtained both low background noise and high spike number of individual spikes. Therefore, we chose the optimal injecting concentration of SPNs-Eu as 1.0×10^4 P/mL for the following sp-ICPMS measurements.

3.5. Optimization of the reaction conditions for Cu^{2+} detection

To sensitively detect the copper ions, several reaction conditions were optimized, including the concentration of SPNs-Eu for reacting with Cu^{2+}, reaction time, and the pH of the reaction solution. As these optimal conditions for detecting Cu^{2+} should be consistent regardless of the final signal readout method, fluorescence method was used to optimize these conditions because of its simplicity. As shown in Fig. 4a, the concentrations of SPNs-Eu were optimized ranging from 0.05 mg/L to 5.0 mg/L. The fluorescence intensity of a certain concentration of SPNs-Eu without the addition of Cu^{2+} was defined as F_0. The fluorescence intensity of the same concentration of SPNs-Eu with the addition of Cu^{2+} (100 μM) was recorded as F. The results showed that the ratio of F/F_0 decreased when the concentration of SPNs-Eu increased from 0.05 mg/L to 1.0 mg/L, and then increased from 1.0 mg/L to 5.0 mg/L. The lowest ratio of F/F_0 at 1.0 mg/L demonstrated the optimal concentration of SPNs-Eu for the detection of copper ions with the highest detection sensitivity, which was used in the followed experiments.

Similarly, the impact of reaction time of SPNs-Eu with Cu^{2+} ions was analyzed by measuring the fluorescence intensity of SPNs-Eu with or without the addition of 100 μM Cu^{2+} in 20 mM HEPES at pH 7.0 by different reaction periods (Fig. 4b). The fluorescence ratio of F/F_0 consistently decreased with the increased reaction time, and reached a plateau after 1.0 h. Therefore, the optimal reaction time of 1.0 h was utilized.

The pH was also an important factor in the aggregation reaction between the Cu^{2+} and SPNs-Eu because pH regulated the forms of the carboxyl groups on the SPNs-Eu. The fluorescence intensity of SPNs-Eu

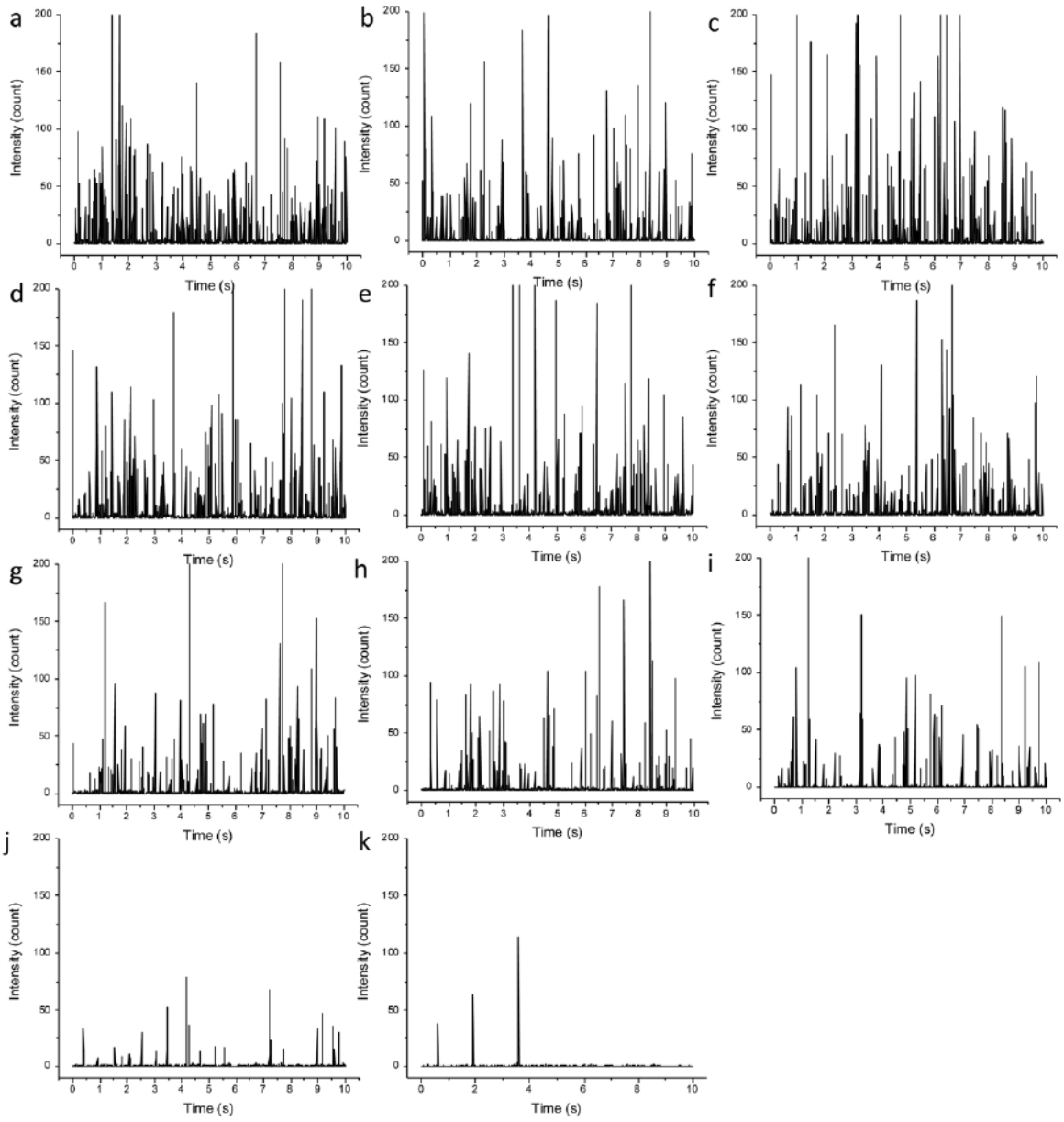

Fig. 7. (a-k) sp-ICPMS profile of SPNs-Eu in the presence of different concentrations of Cu^{2+}(a to k: 0, 0.001, 0.01, 0.1, 1, 10, 100, 1000, 10000, 100000, 1,000,000 nM) incubated in HEPES buffer (20 mM, pH 7.0) at room temperature. The signal of ^{153}Eu was recorded for 180 s with dwell time of 10 ms. The figures here showed a period of 10s' spectra.

mixed with/without Cu^{2+} at different pH were recorded to assess the optimal pH condition. As shown in Fig. 4c, the ratio of F/F_0 decreased as the pH value increased from 1.0 to 7.0 and slightly increased from pH 7.0 to 11.0. Therefore, pH 7.0 was chosen as the optimal pH condition for the detection of Cu^{2+}.

3.6. Detection of Cu^{2+} by fluorometric method

To evaluate the detection limit of the SPNs-Eu for Cu^{2+} using fluorometric method, we performed a titration experiment. Under the optimal conditions, various concentrations of Cu^{2+} (0 μM, 2 μM, 5 μM, 10 μM, 20 μM, 40 μM, 50 μM, 60 μM and 80 μM, respectively) was mixed with 1.0 mg/L SPNs-Eu for 1 h at room temperature in 20 mM HEPES buffer at pH 7.0. The corresponding fluorescence spectra were recorded. As the concentration of Cu^{2+} increased, the fluorescence intensity at 560 nm reduced gradually (Fig. 5A), indicating the fluorescence quenching in the presence of Cu^{2+}. The fluorescence intensity of SPNs-Eu was plotted against the Cu^{2+} concentration (Fig. 5b and c). The results showed that the dynamic range was from 0 μM to 80 μM (Fig. 5b), with a linear range from 2 μM to 50 μM (Fig. 5c). The calibration curve showed a regression equation of $Y = -139.824X + 8442.559$ with a correlation coefficient of 0.992 (Fig. 5c). The limit of detection (LOD) for the detection of Cu^{2+} using the fluorometric method was calculated to be 0.29 μM based on the slope of the equation ($3\sigma/s$), where σ was the standard deviation of three blank fluorescence intensities and s was the slope of the calibration curve. Even this is a relatively high LOD, it could ensure the applicability of the method for the detection of Cu^{2+} in river or drinking water.

3.7. Selectivity of SPNs-Eu by fluorometric method

A selectivity study for Cu^{2+} over different metal ions was performed using the fluorometric method. As shown in Fig. 6, Ni^{2+}, Co^{2+}, Fe^{2+}, Fe^{3+}, Pb^{2+}, Mg^{2+}, Cd^{2+}, Ag^{+}, Zn^{2+}, Al^{3+}, Mn^{2+} were selected in this

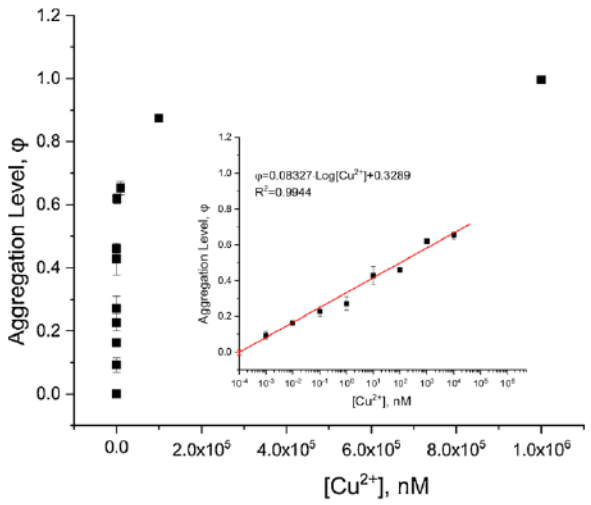

Fig. 8. Relationship between aggregation level (φ) and Cu^{2+} concentration from 0.001 nM to 1,000,000 nM. Inset graph is the calibration curve for Cu^{2+} detection using sp-ICPMS readout in the range of 1.0 pM to 10.0 μM.

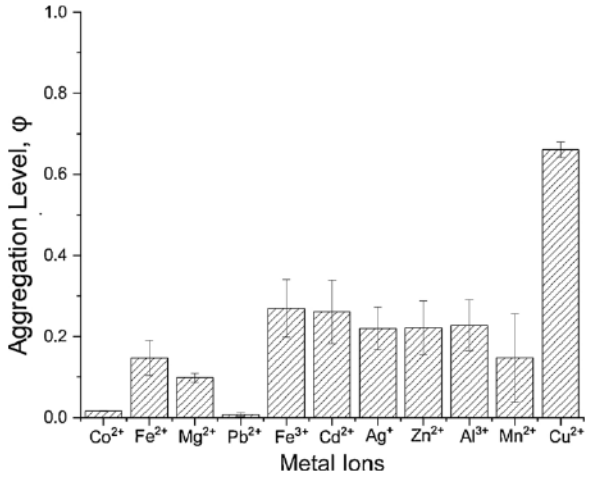

Fig. 9. Selectivity of the SPNs-Eu probe for Cu^{2+} detection by sp-ICPMS. Cu^{2+} and some other ions' concentrations were 1 μM.

Table 2
Spike recovery level of sp-ICPMS and fluorometric methods for Cu^{2+} detection in river water (n = 3).

Methods	Samples	Spiked	Detected	Recovery of this method (%)
SPNs-Eu FL signal	River water (Red river)	10.0 μM	10.3 ± 1.8 (μM)	103 ± 18
Conventional ICP-MS	River water (Red river)	10.0 μM	8.3 ± 0.1 (μM)	83 ± 1
	River water (Red river)	100 nM	89.0 ± 0.6 (nM)	89 ± 1
SPNs-Eu sp-ICPMS signal	River water (Red river)	100 nM	114.8 ± 23.3(nM)	115 ± 23

study. The concentration of these ions was fixed at 50 μM, which were added into 1.0 mg/L of the SPNs-Eu solution in pH 7.0, 20 mM HEPES for 1.0 h. The fluorescence spectra were recorded in the range of 480 nm–700 nm using an excitation wavelength of 480 nm. Compared with other metal ions, the results showed more than 60 % fluorescence quenching when SPNs-Eu were treated with Cu^{2+}, which demonstrated that SPNs-Eu were selective for Cu^{2+} over other metal ions. More interestingly, we found out that both Cd^{2+} and Pb^{2+} showed a little enhanced intensity response instead of decrease. This might be attribute to the bovine serum albumin residues brought in from the filtration process. BSA is a single polypeptide chain containing tryptophan and tyrosine, which have strong affinity to Pb^{2+} and Cd^{2+} [34]. For Pb^{2+}, it can be attributed to the coordination of Pb^{2+} with the pendent carboxylic groups and Nitrogen atoms in BSA, which favors the efficiency of π – π* transition [35]. For Cd^{2+}, it could combine with the surface sulfhydryl groups of BSA@SPN-Eu to form Cd–S bonds, which might facilitate the efficiency of π – π* transition from excited state to ground state [36].

3.8. Copper ion detection by sp-ICPMS

As we discussed previously, the LOD of SPNs-Eu for Cu^{2+} was relatively high (0.29 μM) using the fluorometric method, which could be used in the scenario requiring quick and low-cost detection with relative high concentration of Cu^{2+}, such as in environmental monitoring. However, the sensitivity of the fluorometric method could not satisfy the requirement of trace analysis of Cu^{2+} in the concentration range of nM to pM. In order to break through the limitation of the fluorometric method, we performed the detection of Cu^{2+} using sp-ICPMS method. The feasibility experiments have demonstrated that the number of SPNs-Eu event detected during the sp-ICPMS data collection period (180 s) was decreased in the presence of Cu^{2+} due to the formation of the aggregation (Fig. 2). Therefore, in order to build the relationship between the sp-ICPMS signal with the Cu^{2+} concentration, the aggregation level was defined as aggregation level ϕ in the following Eq. 1.

$$\varphi = 1 - \frac{\text{Number of SPNs} \sim \text{Eu detected } \mathbf{after} \text{ mixed with } Cu^{2+}(E)}{\text{Number of SPNs} \sim \text{Eu detected } \mathbf{before} \text{ mixed with } Cu^{2+}(E_0)} \quad (1)$$

As shown in Fig. 7(a–k), the raw sp-ICPMS profile demonstrated the individual spikes in a wide range of the concentrations of Cu^{2+}covering from 0 nM to 1.0×10^6 nM. With the increase of the concentration of Cu^{2+}, the spike number was dramatically decreased. However, we did not find the obvious enhanced spike intensity, which was supposed to be appeared with the aggregated nanoparticles. We believed that the reason might be the sediment of the aggregated nanoparticles which did not enter the sp-ICPMS system. We plotted the aggregation level with the concentration of Cu^{2+} (Fig. 8). The results showed a linear range of 10^{-3} to 10^4 nM of Cu^{2+}. The regression equation was fitted as $\varphi = 0.08327\text{Log}[Cu^{2+}] + 0.3289$ for Cu^{2+} with a correlation coefficient of 0.9944 (Inset of Fig. 8). The LOD for Cu^{2+} was calculated to be 0.42 pM based on the slope of the equation (3σ/s), where σ was the standard deviation of three blank φ value, and s was the slope of the calibration curve. In conclusion, the sp-ICPMS readout showed a broad linear range and an ultra-low LOD for Cu^{2+} detection.

3.9. Selectivity of SPNs-Eu by sp-ICPMS

The selectivity of the SPNs-Eu probe for Cu^{2+} was also studied using the sp-ICPMS method. A series of metal ions was evaluated including Co^{2+}, Fe^{3+}, Fe^{2+}, Pb^{2+}, Mg^{2+}, Cd^{2+}, Ag^{+}, Zn^{2+}, Al^{3+}, Mn^{2+}, and Cu^{2+} at a concentration of 1 μM. The results were shown in Fig. 9. Compared with other monovalent, bivalent and trivalent metal ions, the aggregation level (φ) of SPNs-Eu in the presence of Cu^{2+} was the highest, indicating the outstanding selectivity of this method for Cu^{2+} detection over other metal ions.

3.10. Analysis of the spiked samples

To test the applicability of SPNs-Eu for Cu^{2+} detection, river water samples were spiked with two different levels of Cu^{2+} (10 μM and 100 nM), followed by detecting both fluorescence signal and sp-ICPMS signal. The high concentration of 10 μM was in the middle of the linear range with fluorometric analysis while nearly out of sp-ICPMS

detection range. In contrast, 100 nM was in the linear range of sp-ICPMS analysis and on the lower end of the linear range of fluorometric method. We supposed to observe the difference in these two concentrations of Cu^{2+} with two different readouts. The spike recovery results from these two readouts are shown in Table 2. The standard traditional ICP-MS method was used as a control. Both the fluorometric method and sp-ICPMS methods showed recoveries ranged from 103 % to 115 %, indicating that these two readouts would be applicable to the detection of with different concentrations and scenarios.

4. Conclusions

In conclusion, we have developed a two-readouts nanoprobe for Cu^{2+} detection by SPNs-Eu. The strong chelating interactions between carboxylic groups and Cu^{2+} induced the aggregation of SPNs-Eu, which induced the fluorescence quenching and reduced spike numbers in sp-ICPMS profile. This two-readouts nanoprobe could satisfy the requirements for the detection of Cu^{2+} in an extremely large range from pM to μM using different readout. Fluorometric method would provide a cost-effective and rapid detection scheme, while sp-ICPMS method would provide a ultras-sensitive and broad linear range detection capacity for Cu^{2+} monitoring. The LODs with fluorometric and sp-ICPMS methods were 0.29 μM and 0.42 pM, respectively. Finally, the SPNs-Eu was also successfully applied for Cu^{2+} detection in river water, demonstrating its applicability for real-sample analysis.

CRediT authorship contribution statement

Dr. Xiao Liu and **Mrs Juan Han** do the experiments and prepare the manuscript. **Dr. Wu** helps to design the experiments and revise the manuscript. **Dr. Julia Xiaojun Zhao** helps to revise the manuscript. **Dr. Pierce David** helps to revise the manuscript.

Declaration of Competing Interest

The authors declare that they have no known competing financial interests or personal relationships that could have appeared to influence the work reported in this paper

Acknowledgments

This work was supported by the NSF grant CHE 1709160 (J.X.Z.) and Applied Research to Address the State's Critical Needs Initiative program of UND (X.W.). We also acknowledge the contribution of Miss. Shuyi He for revising the manuscript, the use of the North Dakota INBRE Metal Analysis Core Facility supported in part by NIH grant 5P20GM103442-18, and the use of the Edward C. Carlson Imaging and Image Analysis Core Facility supported in part by NIH grant 1P30GM103329.

References

[1] B. Fernández, L. Lobo, R. Pereiro, Atomic absorpton spectrometry | Fundamentals, instrumentation and capabilities, in: P. Worsfold, C. Poole, A. Townshend, M. Miró (Eds.), Encyclopedia of Analytical Science, third edition, Academic Press, Oxford, 2019, pp. 137–143.

[2] T.-W. Lin, S.-D. Huang, Direct and simultaneous determination of copper, chromium, aluminum, and manganese in urine with a multielement graphite furnace atomic absorption spectrometer, Anal. Chem. 73 (2001) 4319–4325.

[3] S.L. Bonchin, G.K. Zoorob, J.A. Caruso, Atomic emission, methods and instrumentation, in: J.C. Lindon (Ed.), Encyclopedia of Spectroscopy and Spectrometry, Elsevier, Oxford, 1999, pp. 42–50.

[4] F.R. Abou-Shakra, Chapter 12 - Biomedical applications of inductively coupled plasma mass spectrometry (ICP–MS) as an element specific detector for chromatographic separations, in: I.D. Wilson (Ed.), Handbook of Analytical Separations, Elsevier Science B.V., 2003, pp. 351–371.

[5] A.K. Mahapatra, G. Hazra, N.K. Das, S. Goswami, A highly selective triphenylamine-based indolylmethane derivatives as colorimetric and turn-off fluorimetric sensor toward Cu^{2+} detection by deprotonation of secondary amines, Sens. Actuators B Chem.: Chemical 156 (2011) 456–462.

[6] C.B. Newgard, R.D. Stevens, B.R. Wenner, S.C. Burgess, O. Ilkayeva, M. J. Muehlbauer, et al., Chapter 9 - Comprehensive metabolic analysis for understanding of disease, in: G.S. Ginsburg, H.F. Willard (Eds.), Essentials of Genomic and Personalized Medicine, Academic Press, San Diego, 2010, pp. 97–107.

[7] R.G. Cooks, X. Yan, Mass spectrometry for synthesis and analysis, Annu. Rev. Anal. Chem. 11 (2018) 1–28.

[8] H.N. Wilson, Chapter 13 - Absorptiometry and "colorimetric analysis", in: H. N. Wilson (Ed.), An Approach to Chemical Analysis, Pergamon, 1966, pp. 222–259.

[9] Y. Feng, J. Cheng, L. Zhou, X. Zhou, H. Xiang, Ratiometric optical oxygen sensing: a review in respect of material design, Analyst 137 (2012) 4885–4901.

[10] G. Xu, J. Hou, Y. Zhao, J. Bao, M. Yang, H. Fa, et al., Dual-signal aptamer sensor based on polydopamine-gold nanoparticles and exonuclease I for ultrasensitive malathion detection, Sens. Actuators B Chem. 287 (2019) 428–436.

[11] C.M. McCann, P. Waterman, J.-L. Figueiredo, E. Aikawa, R. Weissleder, J.W. Chen, Combined magnetic resonance and fluorescence imaging of the living mouse brain reveals glioma response to chemotherapy, Neuroimage 45 (2009) 360–369.

[12] Y. Wei, D. Wang, Y. Zhang, J. Sui, Z. Xu, Multicolor and photothermal dual-readout biosensor for visual detection of prostate specific antigen, Biosens. Bioelectron. 140 (2019), 111345.

[13] X. Wu, Q. DeGottardi, I.C. Wu, J. Yu, L. Wu, F. Ye, et al., Lanthanide-coordinated semiconducting polymer dots used for flow cytometry and mass cytometry, Angew. Chem. Int. Ed. 56 (2017) 14908–14912.

[14] E. Petryayeva, W.R. Algar, I.L. Medintz, Quantum dots in bioanalysis: a review of applications across various platforms for fluorescence spectroscopy and imaging, Appl. Spectrosc. 67 (2013) 215–252.

[15] M.J. Ruedas-Rama, J.D. Walters, A. Orte, E.A.H. Hall, Fluorescent nanoparticles for intracellular sensing: a review, Anal. Chim. Acta 751 (2012) 1–23.

[16] H. Prestel, A. Gahr, R. Niessner, Detection of heavy metals in water by fluorescence spectroscopy: on the way to a suitable sensor system, Fresenius J. Anal. Chem. 368 (2000) 182–191.

[17] B.-R. Li, H. Tang, R.-Q. Yu, J.-H. Jiang, Single-nanoparticle ICPMS DNA assay based on hybridization-chain-Reaction-Mediated spherical nucleic acid assembly, Anal. Chem. 92 (2020) 2379–2382.

[18] H. Tapiero, D.M. Townsend, K.D. Tew, Trace elements in human physiology and pathology, Copper, Biomed. Pharmacother. 57 (2003) 386–398.

[19] J. Liu, M. Simms, S. Song, R.S. King, G.P. Cobb, Physiological effects of copper oxide nanoparticles and arsenic on the growth and life cycle of Rice (Oryza sativa japonica 'Koshihikari'), Environ. Sci. Technol. 52 (2018) 13728–13737.

[20] K. Hiroko, F. Chie, B. Wattanaporn, Inherited copper transport disorders: biochemical mechanisms, diagnosis, and treatment, Curr. Drug Metab. 13 (2012) 237–250.

[21] O. Bandmann, K.H. Weiss, S.G. Kaler, Wilson's disease and other neurological copper disorders, Lancet Neurol. 14 (2015) 103–113.

[22] M. DiDonato, B. Sarkar, Copper transport and its alterations in Menkes and Wilson diseases, Biochi. Biophys. Acta (BBA) – Mol. Basis Dis. 1360 (1997) 3–16.

[23] I.V. Muralikrishna, V. Manickam, Chapter One - introduction, in: I. V. Muralikrishna, V. Manickam (Eds.), Environmental Management, Butterworth-Heinemann, 2017, pp. 1–4.

[24] P.B. Tchounwou, C.G. Yedjou, A.K. Patlolla, D.J. Sutton, Heavy metal toxicity and the environment, in: A. Luch (Ed.), Molecular, Clinical and Environmental Toxicology: Volume 3: Environmental Toxicology, Springer Basel, Basel, 2012, pp. 133–164.

[25] C. Ge, J. Chen, W. Wu, Z. Fang, L. Chen, Q. Liu, et al., An enzyme-free and label-free assay for copper(ii) ion detection based on self-assembled DNA concatamers and Sybr Green I, Analyst 138 (2013) 4737–4740.

[26] M. Min, X. Wang, Y. Chen, L. Wang, H. Huang, J. Shi, Highly sensitive and selective Cu^{2+} sensor based on electrospun rhodamine dye doped poly(ether sulfones) nanofibers, Sens. Actuators B Chem. 188 (2013) 360–366.

[27] Y. Dong, R. Wang, G. Li, C. Chen, Y. Chi, G. Chen, Polyamine-functionalized carbon quantum dots as fluorescent probes for selective and sensitive detection of copper ions, Anal. Chem. 84 (2012) 6220–6224.

[28] G.-Y. Lan, C.-C. Huang, H.-T. Chang, Silver nanoclusters as fluorescent probes for selective and sensitive detection of copper ions, Chem. Commun. 46 (2010) 1257–1259.

[29] P.-G. Su, L.-G. Lin, P.-H. Lin, Detection of Cu(II) ion by an electrochemical sensor made of 5,17-bis(4′-nitrophenylazo)-25,26,27,28-tetrahydroxycalix[4]arene-electromodified electrode, Sens. Actuators B Chem. 191 (2014) 364–370.

[30] C. Prado, S.J. Wilkins, F. Marken, R.G. Compton, Simultaneous electrochemical detection and determination of lead and copper at boron-doped diamond film electrodes, Electroanalysis 14 (2002) 262–272.

[31] M. Wang, G. Abbineni, A. Clevenger, C. Mao, S. Xu, Upconversion nanoparticles: synthesis, surface modification and biological applications, Nanomedicine: nanotechnology, Biol. Med. 7 (2011) 710–729.

[32] P.W. Atkins, Shriver & Atkins' Inorganic Chemistry, Oxford University Press, Oxford; New York, 2010.

[33] Y.-H. Chan, Y. Jin, C. Wu, D.T. Chiu, Copper(ii) and iron(ii) ion sensing with semiconducting polymer dots, Chem. Commun. 47 (2011) 2820–2822.

[34] J.S. Mohanty, K. Chaudhari, C. Sudhakar, T. Pradeep, Metal-ion-Induced luminescence enhancement in protein protected gold clusters, J. Phys. Chem. C 123 (2019) 28969–28976.
[35] R. Azadbakht, H. Veisi, H. Mohamadvand, J. Khanabadi, A new fluorescent chemosensor for Pb^{2+} ions based on naphthalene derivatives, Spectrochim. Acta A. Mol. Biomol. Spectrosc. 145 (2015) 575–579.
[36] D. Cheng, X. Liu, Y. Xie, H. Lv, Z. Wang, H. Yang, et al., A ratiometric fluorescent sensor for Cd^{2+} based on internal charge transfer, Sensors Basel (Basel) 17 (2017) 2517.

Xiao Liu is a graduated Ph.D student who is studying in Analytical Chemistry in the University of North Dakota, Grand Forks, ND. Her research mainly focused on silica-based, graphene-based nanomaterials and polymer-based nanomaterials in drug delivery, biosensing and bioanalysis.

Juan Han is a Ph.D candidate student who is majoring in Analytical Chemistry in the University of North Dakota, Grand Forks, ND. Her research focused on nanomaterials in spICP-MS analysis and fluorescent analysis.

Xu Wu is an assistant professor in University of North Dakota, he received his Ph.D degree in 2015 in University of North Dakota and worked in University of Washington as a postdoctoral researcher from 2015 to 2018. His current research is focused on graphene quantum dots, silica nanomaterials, metal nanoparticles, polymer-based nanomaterials, nucleic acids molecules in bioimaging, bioanalysis and biomedical applications.

Julia Xiaojun Zhao is a professor in University of North Dakota in the department of Analytical Chemistry, she received her Ph.D degree in Jilin University in China and worked in Nanoscience & Nanotechnology in University of Florida from 2001 to 2004. She worked as an associated professor from 2009 to 2014 and become a full professor since 2015. Her research focused on metal-based, silica-based, graphene-based nanomaterials and polymer-based nanomaterials in bioimaging, biosensing, catalyst, oil recovery, and biomedical applications.

David Pierce is a professor in University of North Dakota in the department of Analytical Chemistry, his research focuses on nanotechnology, such as fluorescent nanomaterials, photoactive nanomaterials and Nano-catalysts. Recently he started a new project specific targeted on sp-ICPMS technology.